Impulsive forces for haptic rendering of rigid contacts

Daniela Constantinescu
Department of Electrical
and Computer Engineering
University of British Columbia
Vancouver, Canada
Email: danielac@ece.ubc.ca

Septimiu E. Salcudean
Department of Electrical
and Computer Engineering
University of British Columbia
Vancouver, Canada
Email: tims@ece.ubc.ca

Elizabeth A. Croft
Department of
Mechanical Engineering
University of British Columbia
Vancouver, Canada
Email: ecroft@mech.ubc.ca

***Abstract*— This paper presents a haptic rendering method that enables users to feel collisions while they interact with a multi-rigid-body virtual environment through a virtual tool. The virtual tool can be a rigid object or a linkage. Linkage collisions are rendered by extending a collision resolution method proposed for single bodies to articulated structures using a configuration-space representation of dynamics. The configuration-space collision resolution scheme is incorporated into a local model of interaction and used to compute impulsive forces upon contact between the virtual tool and other virtual objects. A four channel teleoperation controller optimized for transparency is used to apply the provably passive impulsive forces to the user's hand. Experiments with a planar rigid virtual world validate the passivity of the impulsive forces.**

I. Introduction

Haptic devices are computer interfaces that allow users to interact with virtual environments through touch and kinesthesia. In many applications, the usefulness of these devices hinges on the realism of the force feedback that they provide. Both the simulation of the virtual environment and the haptic controller contribute to a realistic haptic experience. The simulation computes lifelike interaction forces while the controller transmits these forces to the user's hand faithfully.

Three simulation techniques have been used by prior research to compute physically-motivated interactions with multi-rigid-body virtual environments. Penalty-based methods have been used for haptic interaction with virtual worlds through a virtual tool [1]. Though computationally inexpensive, these methods generate the virtual environment using non-passive algorithms and the interaction may become unstable [2]. Guaranteed stable constraint-based techniques have been developed in [3] and [4]. While these techniques are suitable for point interaction, their extension to rigid body interaction is not straightforward. Haptic manipulation of an impulse-based virtual world has been proposed in [5]. However, both haptic rendering of quasi-static contact and haptic rendering of friction are perceptually unconvincing in the impulse-based virtual environment [5].

Regardless of the technique used for computing the simulated interactions, only penalty-like forces have been rendered to users interacting with multi-rigid-body virtual environments through a virtual tool. These forces reflect the environment stiffness during interactions with penalty-based virtual worlds, and they reflect the stiffness of the virtual coupler during interactions with constraint-based and impulse-based virtual environments. However, psychophysical studies [6], [7] have shown that crisp contacts improve the perceived contact rigidity and that contact crispness is characterized by abrupt forces applied to users upon contact.

To enhance the perceived rigidity of multi-rigid-body virtual worlds, the present research proposes a force model that comprises passive impulsive forces upon contact and penalty and friction forces during contact. This force model is incorporated into a configuration-space formulation of dynamics and used to compute impulsive interactions of virtual linkages. Moreover, the configuration-space collision resolution scheme is included into a local model of interaction, thus enabling the addition of impulsive forces to any multi-rigid-body virtual environment with interactive performance. The impulsive forces are derived employing a new, provably passive, multiple collision resolution technique. Users perceive both the penalty and the impulsive interactions as applied to them by a four-channel teleoperation controller optimized for transparency.

The rest of the paper is organized as follows. The proposed force model is introduced in Section II, followed in Section III by a brief overview of the local model of interaction, including the configuration-space formulation of system dynamics. The passive configuration-space collision resolution scheme is presented in Section IV. Experimental results are given in Section V. Conclusions and directions for future work are discussed in Section VI.

II. The impulsive force model

The present force model is a physically-motivated extension of the "braking pulse" [8] to the haptic manipulation of rigid objects and articulated structures. Designed to provide high damping upon contact, the braking pulse can also be interpreted as the impulsive force arising due to a perfectly plastic point collision. Likewise, the proposed force model includes impulsive forces arising due to multi-rigid-body collisions.

In this model, each contact reported by the collision detection algorithm has three possible states: no contact, colliding contact, and continuous contact, as shown in Figure 1. One time step of the haptic simulation, i.e., one "haptic step", is declared a collision state if one new non-separating contact exists. Non-separating contacts are contacts with negative relative velocity between the contacting bodies along the direction of contact (i.e., with relative velocity inconsistent with the rigidity assumption). During a collision state, all non-separating contacts transition to the collision state. Hence, multiple collisions may occur during one haptic step. They are resolved simultaneously using the method presented in Section IV. During quasi-static contact, the second-order configuration-space dynamics presented in the next section are used to compute the virtual interactions.

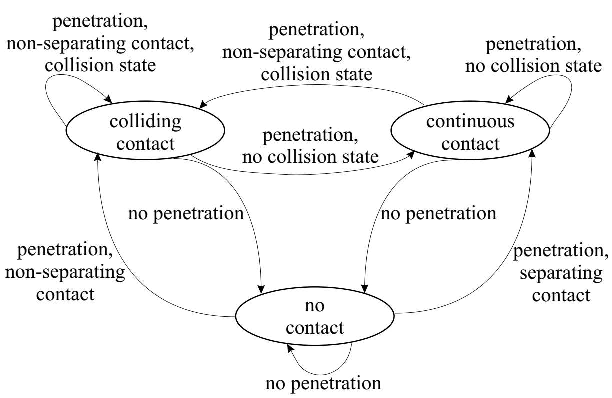

Fig. 1. Contact states according to the proposed force model.

III. The Local Model of Interaction

To enhance the users' perception of rigidity while they manipulate virtual objects and linkages without imposing constraints on the algorithms used to simulate the virtual environment, the force model described above has been incorporated into a local model of interaction [9]. The local model comprises a dynamic proxy of the virtual tool and constraints imposed on the motion of the virtual tool by nearby objects. Manipulation of linkages is incorporated in the local model by defining the virtual tool to be the entire linkage when the user holds one of its links (see Figure 2) and by employing a configuration-space representation of the proxy dynamics. If the virtual tool is a rigid object, its Cartesian-space dynamics are its configuration-space dynamics.

Considering a proxy with d degrees of freedom and c quasi-static contacts, its configuration-space second-order dynamics are:

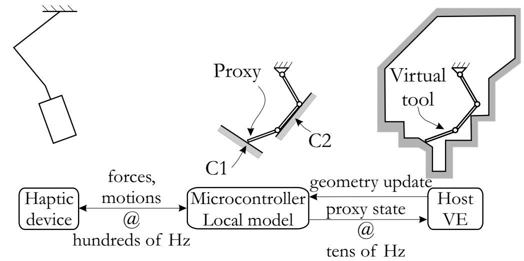

Fig. 2. Local model of interaction comprising a dynamic proxy of a linkage virtual tool and constraints imposed on its motion by nearby objects.

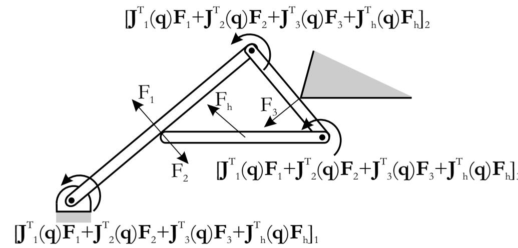

Fig. 3. Example contact and hand forces arising during the haptic manipulation of a linkage proxy with dynamics computed in configuration-space.

$$\begin{aligned}\boldsymbol{D}(\boldsymbol{q})\,\ddot{\boldsymbol{q}} &= -\boldsymbol{B}(\boldsymbol{q},\dot{\boldsymbol{q}}) - \boldsymbol{G}(\boldsymbol{q}) + \\ &\quad + \sum_{i=1}^{c} \boldsymbol{J}_i^T(\boldsymbol{q})\,\boldsymbol{F}_i + \boldsymbol{J}_h^T(\boldsymbol{q})\,\boldsymbol{F}_h. \qquad (1)\end{aligned}$$

In (1), $\boldsymbol{D}(\boldsymbol{q})$ is the configuration space inertia matrix of the system, $\boldsymbol{B}(\boldsymbol{q})$ represent Coriolis and centripetal effects, $\boldsymbol{G}(\boldsymbol{q})$ are the gravitational terms, $\boldsymbol{J}_i(\boldsymbol{q})$ is the Jacobian matrix of the i-th contact, $\boldsymbol{F}_i$ is the contact force at the i-th contact, $\boldsymbol{J}_h(\boldsymbol{q})$ is the Jacobian matrix of the force applied by the user, $\boldsymbol{F}_h$ is the generalized force (force and torque) applied by the user, and $\boldsymbol{q}$, $\dot{\boldsymbol{q}}$, and $\ddot{\boldsymbol{q}}$ are the configuration space positions, velocities, and accelerations, respectively (see Figure 3). Moreover, a contact between two links of the virtual tool, i.e., a "self-contact", is counted twice, once on each link involved in the contact. In the following, the dependence on the instantaneous proxy state of all terms in an equation will be implied.

The contact forces in (1) have a component normal to the constraint plane, $\boldsymbol{F}_{n,i}$, modeling contact rigidity, and a component in the constraint plane, $\boldsymbol{F}_{t,i}$, modeling dry friction:

$$\boldsymbol{F}_i = \boldsymbol{F}_{n,i} + \boldsymbol{F}_{f,i}. \qquad (2)$$

During quasi-static contact, contact rigidity is enforced using penalties:

$$\boldsymbol{F}_{n,i} = -\left(K_{contact}\,p_i + B_{contact}\,v_{n,i}\right)\boldsymbol{n}_i \qquad (3)$$

where $K_{contact}$ and $B_{contact}$ are the contact stiffness and damping, p_i is the penetration between the contacting bodies (positive if the bodies overlap, and zero otherwise), $v_{n,i}$

is the relative velocity of the contacting bodies along the line of contact, and $\boldsymbol{n}_i$ is the contact direction (normal to the constraint plane). The contact direction points towards the proxy at a contact with the environment, and towards the link on which the contact force acts at a self-contact. Dry friction is modeled using a modified Coulomb model:

$$\boldsymbol{F}_{f,i} = \begin{cases} \mu F_{n,i} & \text{if} \quad |v_{t,i}| \geq v_{threshold} \\ \frac{v_{t,i}}{v_{threshold}} \mu F_{n,i} & \text{otherwise} \end{cases} \tag{4}$$

where μ is the coefficient of dry friction for the pair of contacting bodies and $v_{t,i}$ is the relative velocity of the contacting bodies in the constraint plane. The threshold value $v_{threshold}$ allows the contact to transition between stick and slip. From (3), (4) and (1), it can be seen that the contact forces $\boldsymbol{F}_i$ depend only on the proxy state and proxy's acceleration can be directly computed by:

$$\ddot{\boldsymbol{q}} \;=\; \boldsymbol{D}^{-1}\left(-\boldsymbol{B} - \boldsymbol{G} + \sum_{i=1}^{c} \boldsymbol{J}_i^T \boldsymbol{F}_i + \boldsymbol{J}_h^T \boldsymbol{F}_h\right). \tag{5}$$

A fixed step-size integrator is then used during quasi-static contact to advance the proxy state.

When a new non-separating contact arises, the proxy enters a collision state and all non-separating contacts become colliding contacts. The (possibly) multiple collisions are resolved simultaneously using the first-order proxy dynamics, obtained from (1) through integration:

$$\boldsymbol{D}\dot{\boldsymbol{q}} = \boldsymbol{D}\dot{\boldsymbol{q}}_0 + \sum_{i=1}^{c} \boldsymbol{J}_i^T \int_{t_0}^{t} \boldsymbol{F}_i dt. \tag{6}$$

In (6), $\boldsymbol{D}\dot{\boldsymbol{q}}_0$ and $\boldsymbol{D}\dot{\boldsymbol{q}}$ are the pre- and post-collision configuration-space momenta and $\int_{t_0}^{t} \boldsymbol{F}_i dt$ is the collision impulse at the i-th colliding contact. Since the collision is considered instantaneous, i.e., $t \to t_0$, the impulses due to the hand and gravitational forces are negligible. Furthermore, no other external impulses are applied to the proxy apart from the contact impulses. These are computed as outlined in the next section.

IV. Configuration-space collision resolution

In this paper, three assumptions are used to resolve one collision state of the proxy: (i) that the colliding contacts are frictionless; (ii) that all colliding contacts have the same coefficient of restitution, i.e., $e_1 = \cdots = e_c = e$; and (iii) that Newton's restitution hypothesis applies, i.e., the pre- and post-collision normal relative velocities at each contact obey:

$$v_n = -e v_{n_0}, \tag{7}$$

where the index 0 is used for pre-collision quantities and e is the coefficient of restitution. $e \in [0, 1]$ is an empirical constant that describes the behavior of the contact during collision. $e = 1$ describes a perfectly elastic collision, during which the colliding bodies loose no energy. $e = 0$ describes a perfectly plastic collision whereby the colliding bodies do not separate after collision.

Since collisions are assumed frictionless, all contact impulses have components only along the direction of contact:

$$\int_{t_0}^{t} \boldsymbol{F}_i dt = \int_{t_0}^{t} F_i \boldsymbol{n}_i dt = \boldsymbol{n}_i \int_{t_0}^{t} F_i dt = p_i \boldsymbol{n}_i. \tag{8}$$

In (8), $p_i = \int_{t_0}^{t} F_i dt$ is the magnitude of the collision impulse at the i-th frictionless colliding contact. Then, the configuration-space first-order dynamics of the proxy become:

$$\boldsymbol{D}\dot{\boldsymbol{q}} = \boldsymbol{D}\dot{\boldsymbol{q}}_0 + \sum_{i=1}^{c} \boldsymbol{J}_i^T \boldsymbol{n}_i p_i = \boldsymbol{D}\dot{\boldsymbol{q}}_0 + \boldsymbol{\mathcal{J}}_c^T \boldsymbol{p}. \tag{9}$$

In (9), $\boldsymbol{p} = \left(p_1 \ldots p_i \ldots p_c\right)^T$ is the vector of contact impulses and $\boldsymbol{\mathcal{J}}_c = \left[\boldsymbol{J}_1^T \boldsymbol{n}_1 \ldots \boldsymbol{J}_i^T \boldsymbol{n}_i \ldots \boldsymbol{J}_c^T \boldsymbol{n}_c\right]^T$ is the Jacobian matrix of the colliding contacts, i.e., the collision Jacobian. Moreover, c is the number of simultaneous collisions and a collision between two links of the proxy, i.e., a "self-collision", is counted once on each colliding link.

For a proxy with d degrees of freedom and c colliding contacts, (9) represents a set of d equations with $d + c$ unknowns, the post-collision configuration-space velocity $\dot{\boldsymbol{q}}$ and the collision impulses $\boldsymbol{p}$. This system can be solved by augmenting it with Newton's restitution hypothesis.

In configuration-space, (7) becomes:

$$\boldsymbol{n}^T \boldsymbol{J}_i \boldsymbol{q} = -e \boldsymbol{n}^T \boldsymbol{J}_i \boldsymbol{q}_0 \tag{10}$$

at a collision between the proxy and the virtual environment, and:

$$\boldsymbol{n}^T \left(\boldsymbol{J}_i - \boldsymbol{J}_j\right) \boldsymbol{q} = -e \boldsymbol{n}^T \left(\boldsymbol{J}_i - \boldsymbol{J}_j\right) \boldsymbol{q}_0 \tag{11}$$

at a self-collision. (11) imposes a condition only on the relative motion of two links. However, in the local model, this condition is imposed on each link separately:

$$\boldsymbol{n}^T \boldsymbol{J}_i \boldsymbol{q} = -e \boldsymbol{n}^T \boldsymbol{J}_i \boldsymbol{q}_0 \tag{12}$$

and:

$$\boldsymbol{n}^T \boldsymbol{J}_j \boldsymbol{q} = -e \boldsymbol{n}^T \boldsymbol{J}_j \boldsymbol{q}_0. \tag{13}$$

Though more restrictive, (12) and (13) ensure both that Newton's restitution law is observed and that the proposed collision resolution technique is passive, as shown in subsequent derivations. Combining (10), (12), and (13), Newton's restitution law is restated as:

$$\boldsymbol{\mathcal{J}}_c \dot{\boldsymbol{q}} = -e \boldsymbol{\mathcal{J}}_c \dot{\boldsymbol{q}}_0. \tag{14}$$

Equations (9) and (14) describe the first-order dynamics of a proxy with d degrees of freedom and c colliding contacts. Regardless of whether the collisions are non-redundant (i.e., $\boldsymbol{\mathcal{J}}_c$ is full row-rank) or redundant (i.e., $\boldsymbol{\mathcal{J}}_c$ is rank-deficient), the pseudo-inverse of the $\boldsymbol{\mathcal{J}}_c \boldsymbol{D} \boldsymbol{\mathcal{J}}_c^T$ matrix can be used to compute the collision impulses by:

$$\boldsymbol{p} = -\left(1 + e\right) \left(\boldsymbol{\mathcal{J}}_c \boldsymbol{D} \boldsymbol{\mathcal{J}}_c^T\right)^{\dagger} \boldsymbol{\mathcal{J}}_c \dot{\boldsymbol{q}}_0, \tag{15}$$

where $\left(\mathcal{J}_c \boldsymbol{D} \mathcal{J}_c^T\right)^{\dagger} = \left(\mathcal{J}_c \boldsymbol{D} \mathcal{J}_c^T\right)^{-1}$ for non-redundant collisions. These impulses are applied to the user's hand as impulsive forces that change the configuration-space momentum of the proxy over one haptic step by the same amount as the collision impulses:

$$\boldsymbol{F}_{col} = \frac{\mathcal{J}_c^T \boldsymbol{p}}{\Delta t}, \tag{16}$$

where Δt is the time step of the haptic simulation.

The passivity of the proposed collision resolution method (both for non-redundant and for redundant collisions) is shown in the Appendix. Experiments that validate the theoretical results are presented in the next section.

V. EXPERIMENTS

A. System implementation

To validate the theoretical results presented in Section IV, the proposed force model has been implemented in a virtual environment system developed in the Robotics and Control Laboratory at the University of British Columbia. The system comprises a planar haptic interface, a local model of interaction [9] that interfaces the haptic device and the virtual environment simulation, a controller that coordinates both forces and positions between the haptic interface and the local model, and a testbed virtual environment. The virtual environment is generated on a 2.4GHz Pentium IV personal computer running Windows 2000^{TM}, while the local model and the device control are computed on the haptic server, a 700MHz Pentium III personal computer running VxWorks^{TM}. Communication between the two computers is performed via a local area network. A UDP socket is used for inter-process communication, with the local model acting as the server and the virtual environment being the client.

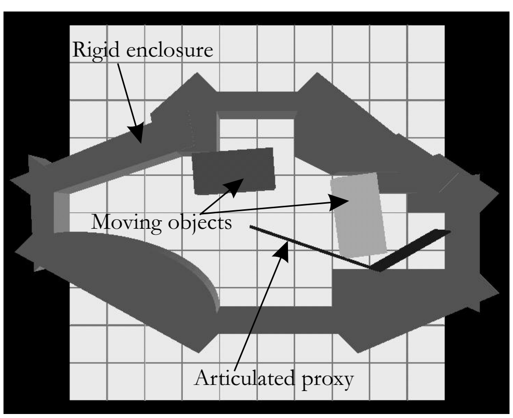

Fig. 4. The testbed virtual environment.

The testbed virtual environment (depicted in Figure 4) is generated using Vortex^{TM}, a physics engine developed by CMLabs Simulations Inc. (www.criticalmasslabs.com). Users can choose interactively any virtual object as the proxy, i.e., the object they manipulate. They feel impulsive forces depending on contact geometry and contact restitution properties when new contacts are formed, and feel the contact stiffness and friction during quasi-static contact.

B. Results

In the experiments, the user manipulates the articulated proxy shown in Figure 4 by holding its third (last) link from its centre of mass. During the manipulation, the linkage comes into contact with the walls of the virtual enclosure and with the other two moving virtual objects. Moreover, neighboring links of the virtual tool obstruct the motion of each other during the experiment.

Two experiments are performed. Perfectly plastic collisions ($e = 0$) are used in the first experiment, while perfectly elastic collisions ($e = 1$) are used in the second one. The number of simultaneous collisions and the change in proxy's kinetic energy during a collision state for both values of the coefficient of restitution are plotted in Figures 5 and 6. The change in kinetic energy is computed by subtracting the proxy's kinetic energy immediately before the impulsive forces are applied to the user's hand from its kinetic energy immediately afterwards. The interaction forces sent to the user are depicted in Figure 7.

The experimental results in Figures 5 and 6 validate the passivity of the proposed collision resolution method. Figure 5 shows that the kinetic energy of the proxy always decreases during plastic collisions, regardless of whether the collisions are non-redundant or redundant. Figure 6 shows that the kinetic energy of the proxy remains constant during elastic collisions (within the limits of numerical accuracy).

The perceptual advantage of the proposed force model can be observed in Figure 7. The impulsive forces are more than an order of magnitude larger than the interaction forces arising during quasi-static contact. Therefore, the acceleration of the user's hand increases correspondingly upon contact and the perceived contact rigidity is enhanced [7].

VI. CONCLUSIONS

In this paper, a haptic rendering method has been proposed that enables users to feel collisions while they interact with multi-rigid-body virtual worlds through a virtual tool. The method incorporates a new force model into a local approximation of the interaction used to interface a haptic device to a virtual environment simulation. The new force model comprises impulsive forces upon contact and penalty and friction forces during impact. The impulsive forces oppose users' intended motion when new contacts arise. They generate large hand accelerations without requiring increased contact stiffness and damping. Impulsive interactions of linkages are rendered by describing the approximate local dynamics in configuration-space. The impulsive interactions are computed using a new, provably passive, multiple collision resolution technique. The technique is non-iterative and compatible with the real-time requirements of haptic applications.

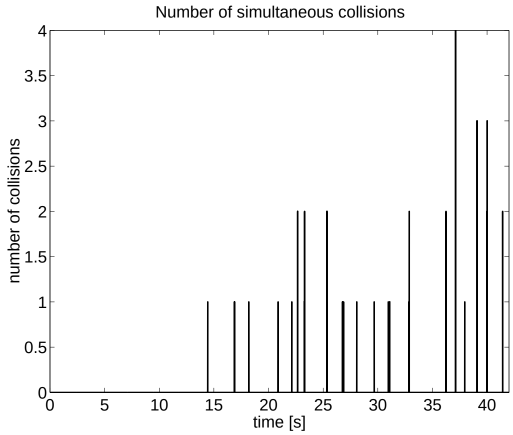

(a)

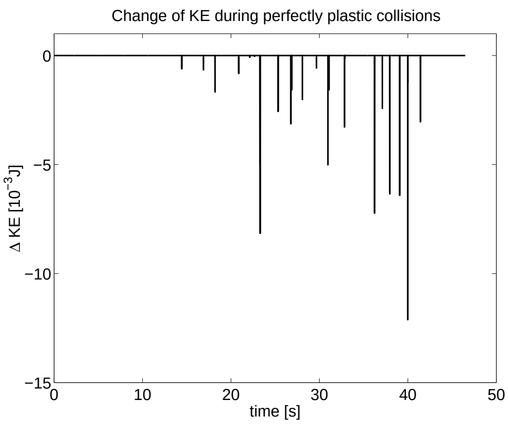

(b)

Fig. 5. The change of the kinetic energy (KE) of the linkage proxy during collisions with perfectly plastic ($e = 0$) walls and objects.

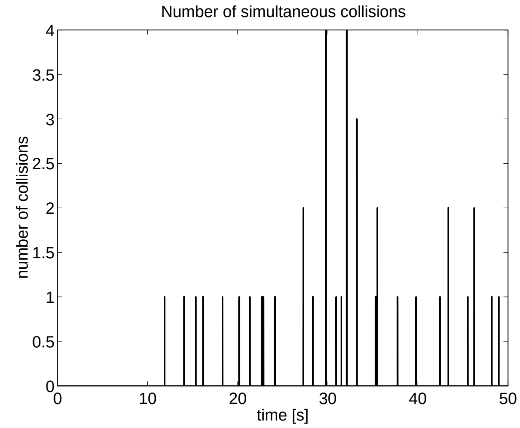

(a)

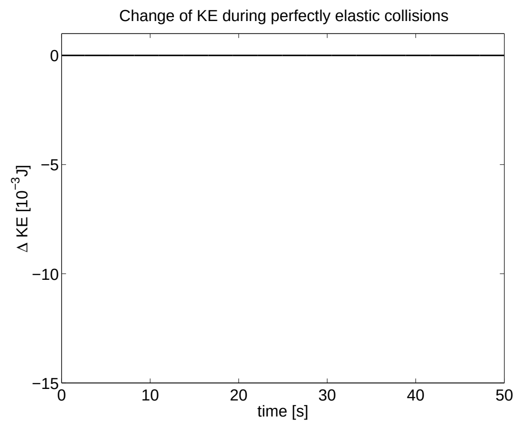

(b)

Fig. 6. The change of the kinetic energy (KE) of the linkage proxy during collisions with perfectly elastic ($e = 1$) walls and objects.

Work under way includes the extension of the proposed collision resolution scheme to multiple colliding contacts with varying restitution properties and to the interaction with deformable objects.

VII. Appendix

In this appendix, it is shown that the kinetic energy of a d degrees of freedom proxy with c colliding contacts (either non-redundant or redundant) does not increase during a collision state if the collision state is resolved using (15).

For non-redundant collisions, the post-collision velocity of the proxy is:

$$\dot{\boldsymbol{q}} = \dot{\boldsymbol{q}}_0 - (1+e)\,\overline{\boldsymbol{\mathcal{J}}}_c\boldsymbol{\mathcal{J}}_c\dot{\boldsymbol{q}}_0 = \left(\boldsymbol{I} - (1+e)\,\overline{\boldsymbol{\mathcal{J}}}_c\boldsymbol{\mathcal{J}}_c\right)\dot{\boldsymbol{q}}_0, \tag{17}$$

where $\overline{\boldsymbol{\mathcal{J}}}_c = \boldsymbol{D}^{-1}\boldsymbol{\mathcal{J}}_c^T\left(\boldsymbol{\mathcal{J}}_c\boldsymbol{D}^{-1}\boldsymbol{\mathcal{J}}_c^T\right)^{-1}$ is the dynamically consistent inverse of the collision Jacobian [10]. Using the definition of $\overline{\boldsymbol{\mathcal{J}}}_c$, the symmetry of $\boldsymbol{D}$, and some algebraic manipulation, it can be shown that:

$$\left(\boldsymbol{I} - \boldsymbol{\mathcal{J}}_c^T\overline{\boldsymbol{\mathcal{J}}}_c^T\right)\boldsymbol{D}\overline{\boldsymbol{\mathcal{J}}}_c\boldsymbol{\mathcal{J}}_c = \boldsymbol{\mathcal{J}}_c^T\overline{\boldsymbol{\mathcal{J}}}_c^T\boldsymbol{D}\left(\boldsymbol{I} - \overline{\boldsymbol{\mathcal{J}}}_c\boldsymbol{\mathcal{J}}_c\right) = \boldsymbol{0}. \tag{18}$$

Then, it follows that:

$$\begin{aligned}
&\left(\boldsymbol{I} - \boldsymbol{\mathcal{J}}_c^T\overline{\boldsymbol{\mathcal{J}}}_c^T\right)\boldsymbol{D}\overline{\boldsymbol{\mathcal{J}}}_c\boldsymbol{\mathcal{J}}_c + \boldsymbol{\mathcal{J}}_c^T\overline{\boldsymbol{\mathcal{J}}}_c^T\boldsymbol{D}\left(\boldsymbol{I} - \overline{\boldsymbol{\mathcal{J}}}_c\boldsymbol{\mathcal{J}}_c\right) = \boldsymbol{0}\\
&\Rightarrow \boldsymbol{D}\overline{\boldsymbol{\mathcal{J}}}_c\boldsymbol{\mathcal{J}}_c + \boldsymbol{\mathcal{J}}_c^T\overline{\boldsymbol{\mathcal{J}}}_c^T\boldsymbol{D} = 2\boldsymbol{\mathcal{J}}_c^T\overline{\boldsymbol{\mathcal{J}}}_c^T\boldsymbol{D}\overline{\boldsymbol{\mathcal{J}}}_c\boldsymbol{\mathcal{J}}_c\\
&\Rightarrow (1+e)\,\dot{\boldsymbol{q}}_0^T\left(\boldsymbol{D}\overline{\boldsymbol{\mathcal{J}}}_c\boldsymbol{\mathcal{J}}_c + \boldsymbol{\mathcal{J}}_c^T\overline{\boldsymbol{\mathcal{J}}}_c^T\boldsymbol{D}\right)\dot{\boldsymbol{q}}_0 =\\
&2\,(1+e)\,\dot{\boldsymbol{q}}_0^T\boldsymbol{\mathcal{J}}_c^T\overline{\boldsymbol{\mathcal{J}}}_c^T\boldsymbol{D}\overline{\boldsymbol{\mathcal{J}}}_c\boldsymbol{\mathcal{J}}_c\dot{\boldsymbol{q}}_0\\
&\geq (1+e)^2\,\dot{\boldsymbol{q}}_0^T\boldsymbol{\mathcal{J}}_c^T\overline{\boldsymbol{\mathcal{J}}}_c^T\boldsymbol{D}\overline{\boldsymbol{\mathcal{J}}}_c\boldsymbol{\mathcal{J}}_c\dot{\boldsymbol{q}}_0 \quad \forall e \in [0,1]\\
&\Rightarrow \dot{\boldsymbol{q}}_0^T\boldsymbol{D}\dot{\boldsymbol{q}}_0 \geq \dot{\boldsymbol{q}}_0^T\boldsymbol{D}\dot{\boldsymbol{q}}_0 -\\
&(1+e)\,\dot{\boldsymbol{q}}_0^T\boldsymbol{D}\overline{\boldsymbol{\mathcal{J}}}_c\boldsymbol{\mathcal{J}}_c\dot{\boldsymbol{q}}_0 - (1+e)\,\dot{\boldsymbol{q}}_0^T\boldsymbol{\mathcal{J}}_c^T\overline{\boldsymbol{\mathcal{J}}}_c^T\boldsymbol{D}\dot{\boldsymbol{q}}_0 +\\
&(1+e)^2\,\dot{\boldsymbol{q}}_0^T\boldsymbol{\mathcal{J}}_c^T\overline{\boldsymbol{\mathcal{J}}}_c^T\boldsymbol{D}\overline{\boldsymbol{\mathcal{J}}}_c\boldsymbol{\mathcal{J}}_c\dot{\boldsymbol{q}}_0 \quad \forall e \in [0,1],
\end{aligned} \tag{19}$$

and, by re-arranging terms:

$$\begin{aligned}
&\dot{\boldsymbol{q}}_0^T\boldsymbol{D}\dot{\boldsymbol{q}}_0 \geq\\
&\dot{\boldsymbol{q}}_0^T\left(\boldsymbol{I} - (1+e)\,\overline{\boldsymbol{\mathcal{J}}}_c\boldsymbol{\mathcal{J}}_c\right)^T\boldsymbol{D}\left(\boldsymbol{I} - (1+e)\,\overline{\boldsymbol{\mathcal{J}}}_c\boldsymbol{\mathcal{J}}_c\right)\dot{\boldsymbol{q}}_0\\
&\Rightarrow \dot{\boldsymbol{q}}_0^T\boldsymbol{D}\dot{\boldsymbol{q}}_0 \geq \dot{\boldsymbol{q}}^T\boldsymbol{D}\dot{\boldsymbol{q}}.
\end{aligned} \tag{20}$$

Hence, for any value of the coefficient of restitution, the post-collision kinetic energy of the proxy is at most

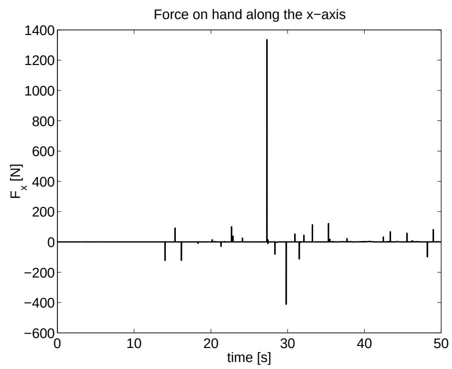

(a)

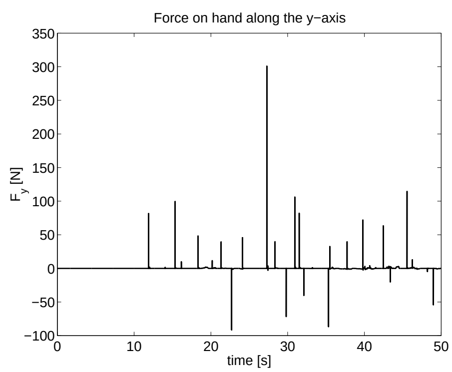

(b)

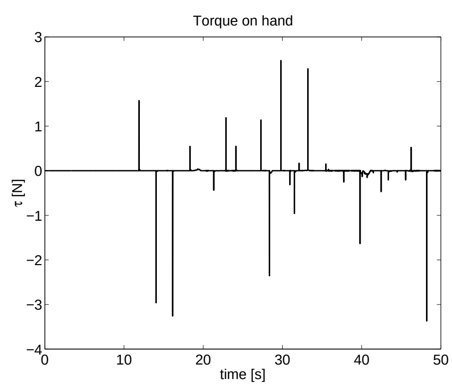

(c)

Fig. 7. Contact forces and torques applied on the user's hand during the manipulation of the linkage proxy in a virtual environment with perfectly elastic collisions ($e = 1$).

equal to its pre-collision kinetic energy. If the simultaneous collisions are perfectly elastic, i.e., $e = 1$, then the kinetic energy of the proxy does not change during a collision state, since:

$$\begin{aligned}\dot{\boldsymbol{q}} &= \dot{\boldsymbol{q}}_0 - 2\overline{\boldsymbol{\mathcal{J}}}_c\boldsymbol{\mathcal{J}}_c\dot{\boldsymbol{q}}_0 = \\ &= \dot{\boldsymbol{q}}_0 - 2\boldsymbol{D}^{-1}\boldsymbol{\mathcal{J}}_c^T\left(\boldsymbol{\mathcal{J}}_c\boldsymbol{D}^{-1}\boldsymbol{\mathcal{J}}_c^T\right)^{-1}\boldsymbol{\mathcal{J}}_c\dot{\boldsymbol{q}}_0 = \\ &= \dot{\boldsymbol{q}}_0 - 2\dot{\boldsymbol{q}}_0 = -\dot{\boldsymbol{q}}_0.\end{aligned} \tag{21}$$

If the simultaneous collisions are redundant, the post-collision velocity of the proxy is:

$$\dot{\boldsymbol{q}} = \dot{\boldsymbol{q}}_0 - (1+e)\left(\boldsymbol{\mathcal{J}}_c\boldsymbol{D}^{-1}\boldsymbol{\mathcal{J}}_c^T\right)^{\dagger}\boldsymbol{\mathcal{J}}_c\dot{\boldsymbol{q}}_0. \tag{22}$$

To show that the resolution of redundant collisions is passive, the same reasoning as outlined in (18)-(20) can be followed after substituting $\left(\boldsymbol{\mathcal{J}}_c\boldsymbol{D}^{-1}\boldsymbol{\mathcal{J}}_c^T\right)^{\dagger}$ for $\left(\boldsymbol{\mathcal{J}}_c\boldsymbol{D}^{-1}\boldsymbol{\mathcal{J}}_c^T\right)^{-1}$. The proof holds because:

$$\begin{aligned}&\left(\boldsymbol{\mathcal{J}}_c\boldsymbol{D}^{-1}\boldsymbol{\mathcal{J}}_c^T\right)^{\dagger} = \\ &= \left(\boldsymbol{\mathcal{J}}_c\boldsymbol{D}^{-1}\boldsymbol{\mathcal{J}}_c^T\right)^{\dagger}\boldsymbol{\mathcal{J}}_c\boldsymbol{D}^{-1}\boldsymbol{\mathcal{J}}_c^T\left(\boldsymbol{\mathcal{J}}_c\boldsymbol{D}^{-1}\boldsymbol{\mathcal{J}}_c^T\right)^{\dagger}.\end{aligned} \tag{23}$$

REFERENCES

[1] A. Gregory, A. Mascarenhas, S. Ehmann, M. Lin, and D. Manocha, "Six Degree-of-Freedom Haptic Display of Polygonal Models," in *Proceedings Visualization 2000*, 2000, pp. 139–146.

[2] J. Colgate, M. Stanley, and J. Brown, "Issues in the Haptic Display of Tool Use," in *Proceedings of the IEEE/RSJ International Conference on Intelligent Robots and Systems*, Pittsburgh, 1995, pp. 140–145.

[3] C. Zilles and J. Salisbury, "A Constraint-based God Object Method for Haptic Display," in *ASME Haptic Interfaces for Virtual Environment and Teleoperator Systems, Dynamic Systems and Control*, Chicago, IL, 1994, pp. 146–150.

[4] D. Ruspini, K. Koralov, and O. Khatib, "The Haptic Display of Complex Graphical Environments," in *Proceedings of the SIGGRAPH 97*, Los Angeles, CA, 1997, pp. 345–352.

[5] B. Chang and J. Colgate, "Real-Time Impulse-Based Simulation of Rigid Body Systems for Haptic Display," in *Proceedings of the 1997 ASME International Mechanical Engineering Congress and Exhibition*, Dallas, Texas, 1997, pp. 1–8.

[6] L. Rosenberg and B. Adelstein, "Perceptual Decomposition of Virtual Haptic Surfaces," in *Proceedings of the IEEE Symposium on Research Frontiers in Virtual Reality*, Los Alamitos CA, 1993, pp. 46–53.

[7] D. Lawrence, L. Pao, A. Dougherty, M. Salada, and Y. Pavlou, "Rate-Hardness: A New Performance Metric for Haptic Interfaces," *IEEE Transactions on Robotics and Automation*, vol. 16, no. 4, pp. 357–371, 2000.

[8] S. Salcudean and T. Vlaar, "On the Emulation of Stiff Walls and Static Friction with a Magnetically Levitated Input/Output Device," *ASME Journal of Dynamics, Measurement and Control*, vol. 119, pp. 127–132, March 1997.

[9] D. Constantinescu, S. Salcudean, and E. Croft, "Haptic Feedback using Local Models of Interaction," in *11th International Symposium on Haptic Interfaces for Virtual Environment and Teleoperator Systems*, Los Angeles, CA, 2003, pp. 416–421.

[10] O. Khatib, "Inertial Properties in Robotic Manipulation: An Object-Level Framework," *The International Journal of Robotics Research*, vol. 13, no. 1, pp. 19–36, 1995.